UNIVERSITY OF CALIFORNIA, IRVINE

Air SHIELD: Aircraft Structural Health Intelligence for Evaluation and Lifecycle Detection

Written by:
Oi Ching Vanessa Chung, *PhD student, Mechanical and Aerospace Engineering, University of California, Irvine*

Bryce M. Mankovsky, *Senior, Mechanical and Aerospace Engineering, University of California, Irvine*

Addison Rushing, *Senior, Mechanical Engineering, University of California, Irvine*

Jerry Chen, *Junior, Mechanical Engineering and Mathematics, University of California, Irvine*

Advised by:
Jacqueline Huynh, *Assistant Professor, Department of Mechanical and Aerospace Engineering, University of California, Irvine*

NASA Blue Skies Competition
RepAir: Advancing Aircraft Maintenance

May 3, 2026

Air SHIELD:
Aircraft Structural Health Intelligence for Evaluation and Lifecycle Detection

Project Summary:

Case studies show **Air SHIELD** saves $9.13 per flight hour, $444,932 over an aircraft's lifetime, and adds 570 hours of utilization, while keeping aircraft safer and more available. This revolutionary and autonomous structural health monitoring system continuously detects, locates, and classifies damage in real time. By combining advanced sensors, physics-based models, and machine learning, it reduces routine inspections and unplanned maintenance, and delivers smarter operations, faster turnarounds, and lower costs. It positions operators to meet the demands of sustainable, high-utilization aviation while enabling data-driven maintenance decisions across the fleet.

Project Image

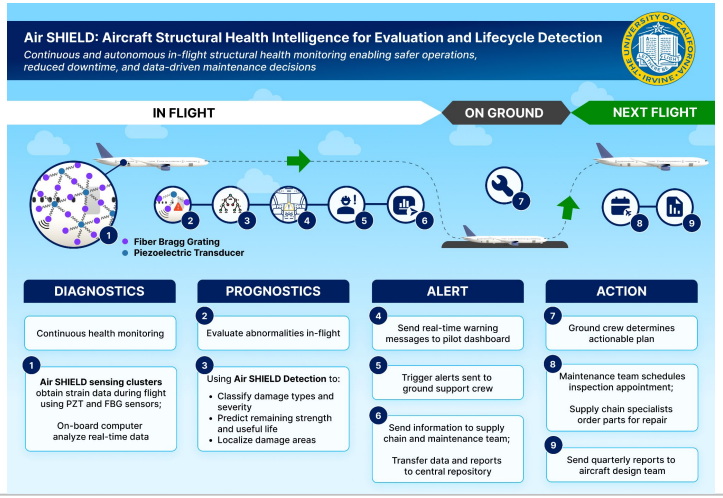

Team Composition:

University of California, Irvine

Aircraft Systems Laboratory

Oi Ching Vanessa Chung – PhD student, Mechanical and Aerospace Engineering

Bryce M. Mankovsky – Senior, Mechanical and Aerospace Engineering

Addison Rushing – Senior, Mechanical Engineering

Jerry Chen – Junior, Mechanical Engineering and Mathematics

At UC Irvine's Aircraft Systems Laboratory, we create innovative solutions to advance sustainable aviation, optimize operations, integrate emerging technologies, and minimize environmental impacts across the airspace.

Project Timeline

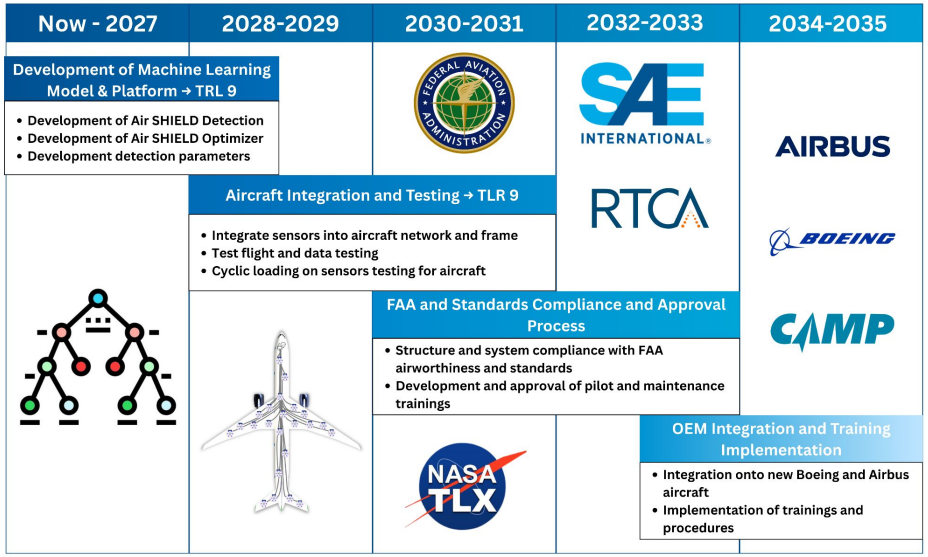

This proposal introduces **Air SHIELD**, a hybrid structural health monitoring technology enabling continuous, autonomous assessment of aircraft structures during flight. Unlike current manual inspection methods using flashlights, cameras, or acoustic techniques, **Air SHIELD** provides real-time data on structural integrity, reducing the risk of undetected damage and minimizing aircraft downtime. Our work focuses on optimizing the sensor architecture and developing a sophisticated machine learning model for accurate damage detection, localization, and remaining useful life prediction. This is done by introducing **Air SHIELD Sensing Cluster**, composed of piezoelectric transducers that generate guided waves across the aircraft surface, and received by fiber Bragg gratings sensor, with placement informed by **Air SHIELD Optimizer**. Damage alters the wave propagation, producing measurable wavelength shifts that indicate strain. **Air SHIELD Detection** is a graph neural network that processes the sensor data and performs global damage detection, point-wise localization, damage type classification, and remaining useful life prediction. Planned experimental validation with representative structures confirms simulation accuracy, sensor performance, and the effectiveness of sensor placement optimization.

To reduce system mass while maintaining measurement fidelity, a zonal interrogation strategy divides the sensor network into three zones, lowering equipment weight by approximately 5.5 times. When applied to a 737 NG, the addition of **Air SHIELD** increases empty operating weight by 0.2%, but creates a net savings of $9.13 per flight hour, by reducing maintenance cost. Across the aircraft's operational lifetime, the implemented system saves the operator $444,932, while also increasing the aircraft's utilization by 570 hours. The proposal also defines the development, testing, and validation steps required to achieve operational deployment by 2035. By combining advanced sensing, predictive modeling, and a structured and systematic implementation plan, this approach supports continuous diagnostics, prognostics, and autonomous alerting, improving safety, maintenance efficiency, and operational decision-making for aircraft.

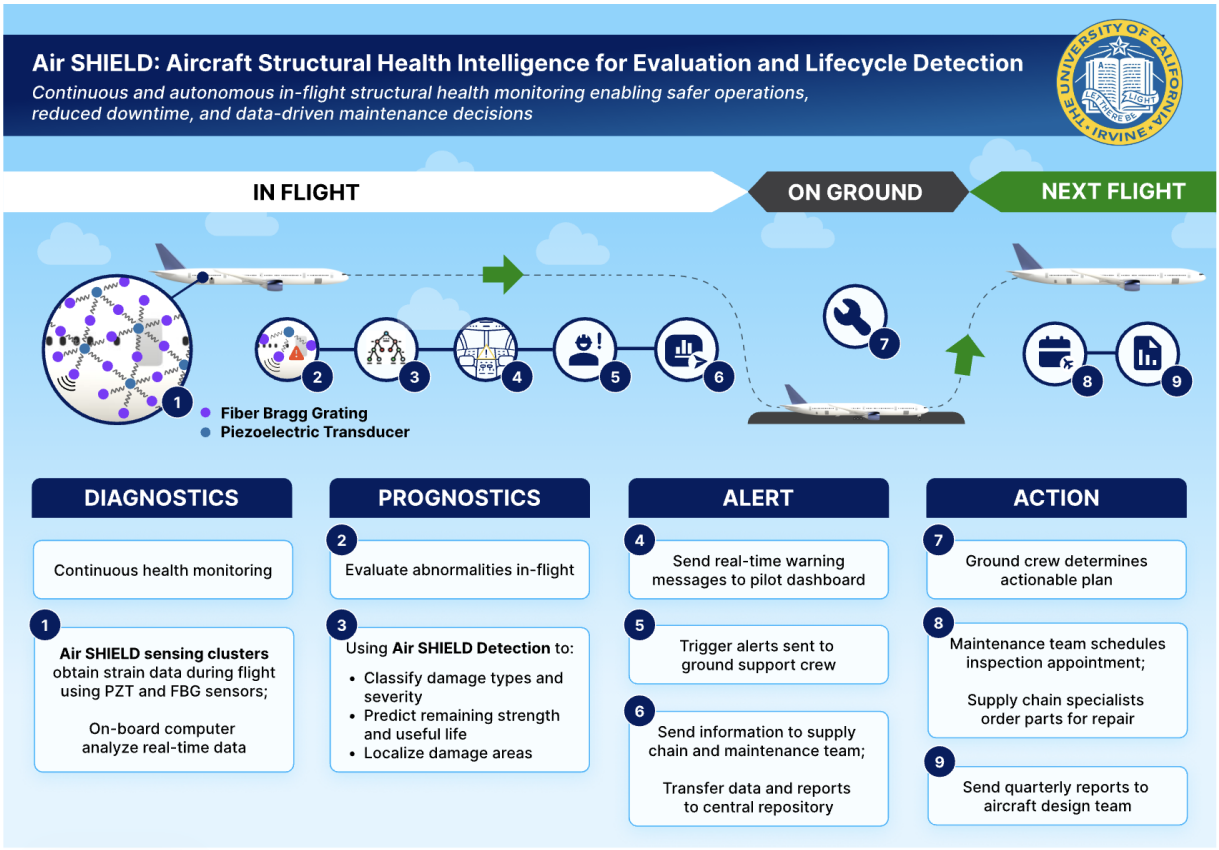

1 Situational Assessment

Safety is of the utmost importance when it comes to aviation. According to the FAA FAR 25.571, the structure of the aircraft must retain its structural strength during the operational life after it has sustained a given level of fatigue, corrosion, and accidental damage [1]. In aviation, structural damage can be categorized into three primary types: accidental damage, environmental deterioration, and fatigue damage [2], with description highlighted in Table A.1 in the Appendix. Structural health monitoring (SHM) is important because it reflects the health status of a structure, thereby informing engineers of its life-time, damage states, and locations so that maintenance can be scheduled and performed to prevent damage from further propagating. The general practice that airlines currently adhere to is a periodic maintenance schedule, where aircraft are inspected at intervals of months, and manual visual inspections are performed with the assistance of a flashlight by technicians to determine and detect damages or deformation [3, 4]. This is highly subjective; it can lead to human error and doesn't collect any data related to the inspection or condition of the aircraft. Additionally, while advanced warning and monitoring systems have been implemented on Generation 3 and 4 transport aircraft for automated warning cues, diagnostics time and human workload actually increases during non-normal scenarios where only subtle and ambiguous failures or cues are available [5, 6]. One example is the 1988 accident involving an aircraft operated by Aloha Airlines in the Hawaii region, which had undergone repeated fatigue loading due to numerous short-haul flights between the Hawaiian Islands, causing internal damage that remained difficult to detect during routine inspections. These repeated fatigue cycles weakened the material internally, ultimately causing a portion of the fuselage roof to rupture [7].

Currently, the only existing aircraft that has SHM on-board is the F-35 [8]. Despite the enterprise maturity of the F-35 SHM, the on-board structural sensing does not provide guided wave non-destructive evaluation (NDE), a capability that is crucial for early, local detection and sizing of barely visible impact damage (BVID), disbonds, and small cracks that rarely perturb global strain at sparse gauge locations. As SHM scales to larger airframes, simply multiplying low-bandwidth strain gauges increases complexity without commensurate coverage. Airbus and Boeing also have their respective predictive health monitoring platforms to support aircraft maintenance and operations across airlines but this ecosystem primarily monitors systems health states and has limited information on monitoring the structural health of the aircraft [9–11].

Given the health monitoring gaps in commercial aviation, our objective is to highlight the prognostics and diagnostics technology and benefits of incorporating strain gauges and transducers to continuously acquire strain data used for detecting and classifying damage types, severity, and remaining useful life. This approach allows for continuous health monitoring during flight operations, increases decision making efficiency, reduces operational downtime, and lowers maintenance costs for condition-based inspection.

2 Solution: Air SHIELD Sensing Cluster, Optimizer, and Detection

A data-driven predictive structural health monitoring system requires coordinated front-end and back-end development. The Back-end focuses on mechanical integration and sensing technologies that enable prognostic and diagnostic capabilities. The Front-end, described in Section 3.1, involves coordination among multiple stakeholders to enable reliable data transfer, processing, and analysis across the system architecture. Our proposed solution, **Air SHIELD**, integrates hybrid strain sensing hardware, specifically fiber Bragg grating (FBG) sensors and piezoelectric transducers (PZT), forming **Air SHIELD Sensing Clusters** with placement determined by the **Air SHIELD Optimizer**, onto aircraft structures to continuously measure strain variations. The data serve as inputs for the damage detection, localization, and prediction algorithms called **Air SHIELD Detection**. This combined approach reduces uncertainties related to potential structural damage caused by fatigue, environmental deterioration, or unplanned impact scenarios, especially for early detection of BVID, a critical form of internal damage in composite materials that is not externally visible and can significantly reduce material integrity and overall structural strength.

2.1 Air SHIELD Sensing Cluster

The **Air SHIELD Sensing Cluster**, displayed in Fig.2.1, integrates PZT and FBG sensors for guided wave sensing. A voltage input excites the PZT, generating guided elastic waves at a selected frequency that propagate through the structure, attenuating with distance and material damping, and are received by FBG sensors that measure the dynamic strain response. Each FBG sensor consists of a periodic grating inscribed in an optical fiber that reflects Bragg wavelength from a broadband light source. Mechanical strain alters the grating period, producing a measurable shift in the reflected wavelength relative to the initial equilibrium state. An optical interrogator tracks this shift and converts it to strain using calibrated relationships. Prior studies by [12, 13] validated this hybrid concept under controlled laboratory conditions.

The **Air SHIELD Sensing Cluster** is revolutionary because it enables global assessment of structural damage rather than isolated point measurements. An FBG sensor used alone measures strain over a limited sensing region near the bonded location. When paired with PZT, guided elastic waves travel across the structure and interact with discontinuities such as cracks or delaminations. Damage alters wave amplitude and propagation characteristics, which appear as measurable wavelength shifts in the FBG response. This behavior supports early detection over a larger inspection area. The small size and low mass of both sensors support aircraft integration, where added mass affects thrust, engine selection, and vehicle performance. Additional mass may also require structural reinforcement, which further increases weight and aerodynamic drag. Moreover, the multiplexing capability of FBG sensors enables multiple sensing locations along a single optical fiber, reducing wiring complexity and minimizing the amount of onboard electronics required for data acquisition [3, 14].

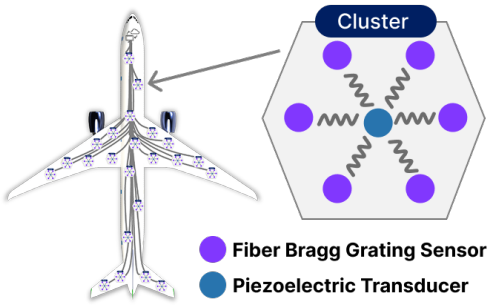

Figure 2.1: Air SHIELD Sensing Cluster

2.2 Air SHIELD Optimizer for Sensor Placement

Sensor installation on aircraft structures requires two tightly coupled steps: sensor placement optimization (SPO) and damage detection and classification. The location of each FBG sensor or PZT on a panel determines how sensitively it records the strain variations that occur during flight; therefore, sensors must be placed preferentially in regions of high strain and stress. Because exhaustive trial-and-error testing of thousands of possible layouts would demand an impractical amount of finite element modeling (FEM) and flight test time, the placement problem must be addressed with a principled, data-driven design methodology.

Studies have scrutinized different methods for determining sensors locations, but they focused on controllability and observability rather than direct damage detection [15–24]. More efficiently, **Air SHIELD Optimizer** adopts a **design-amortized Bayesian Optimal Experimental Design** (BOED) approach. Instead of optimizing each layout independently, it trains a single variational model once and reuses it to evaluate the expected information gain (EIG) for a large design space using the Variational Nested Monte Carlo (VNMC) bound tightening strategy [25, 26], enabling the trained model to evaluate new layouts without repeated retraining. It significantly reduces FEM requirement and lowers computational cost while improving efficiency in identifying sensor locations based on prior knowledge of high strain and stress regions.

The development of **Air SHIELD Optimizer** begins with defining the design variables, including discrete mesh coordinates and orientation. Latent parameters represent damage characteristics, including location, size, severity, and type. The model also accounts for uncertainties to better represent operational conditions, such as atmospheric variation, boundary condition uncertainty, sensor noise and failure probability, and bonding degradation between the sensor and the structure. These uncertainties are incorporated through baseline calibration datasets that account for environmental variation, weighted risk factors assigned to potential sensor failures, and extensive FEM simulations across multiple loading and flight conditions to

represent realistic structural responses. Wave characteristics, including sensing range and propagation behavior, are incorporated as it affects coverage and layout feasibility across the surface. The addition of operational uncertainties and wave characteristics into a SPO has never been studied extensively before.

Prior knowledge for **Air SHIELD Optimizer** is introduced through a large set of simulated FEM representing realistic flight loads, operating conditions, and damage scenarios and highlight structurally significant regions. During training, a variational bound is used to learn the amortized posterior and VNMC is applied to tighten the bounds on EIG for each candidate layout, improving reliability in design ranking and selection. Design evaluation uses a risk-weighted utility that rewards information gain while penalizes missed detections in critical regions and false alarms that drive unnecessary maintenance actions. Once trained, the model supports fast, repeatable layout optimization without re-running large numbers of FEM.

2.2.1 Damage Types and Numerical Representation

Each damage mechanism produces distinct geometric features and stress distributions that influence strain response and guided wave behavior. Accurate representation of these physical characteristics is required to provide meaningful inputs to the damage classification model and improve identification accuracy. Table 2.1 summarizes representative damage mechanisms, physical effects, and data acquisition method for developing **Air SHIELD Optimizer** and **Detection** using FEM and experimental tests. Fig. A.2 in the Appendix illustrates the inputs and outputs workflow from FEM and experimental data.

Damage Type	**Physical Response on Structures**	**Data Acquisition Methods**
Low-velocity impact (Accidental Damage)	Local plastic deformation, surface denting, residual stress; no cracking at medium energy	Drop-weight impact simulation; explicit dynamics with elastic-plastic material model; post-impact residual stress field retained as initial condition
High-velocity impact / penetration (Accidental Damage)	Severe plastic deformation, cracking, perforation, material loss	Johnson--Cook constitutive and damage model with element erosion (e.g. LS-DYNA); validation via ballistic limit and perforation morphology
Pitting corrosion	Localized section loss and sharp stress concentrations; early local plasticity	Surface notches or pits introduced geometrically; combined with initial stress fields to represent corrosion-induced weakening
Long-term corrosion	Reduction of effective load-bearing area; global stiffness degradation	Local thickness reduction of structural components
Fatigue cracking	Crack initiation and growth; strong stress concentration and crack-tip plasticity	Predefined strip-shaped crack with applied initial stress field at crack tip to mimic fatigue damage effects

Table 2.1: Summary of damage types, physical material response, and data acquisition methods

2.2.2 Air SHIELD for Corrosion Detection

Corrosion are high-value targets for **Air SHIELD** because it can begin as localized material changes before producing clear visual indications. Pitting corrosion introduces local section loss and stress concentration, and long-term corrosion reduces effective load-bearing area and stiffness. These damage modes are difficult to detect visually when they occur near fasteners, on backside surfaces, or in stiffened regions. Corrosion studies conducted by NASA noted that corrosion is often identified only after visible surface distortion, such as pillowing, while inaccessible regions require advanced NDT methods [27]. Corrosion under coating may also remain hidden until blistering, cracking, or coating failure appears [28].

Prior studies show strong potential for guided-wave sensing to detect hidden corrosion and back-surface corrosion in aluminum [29, 30]. Piezoelectric wafer active sensor networks have also detected opposite-side material loss in aluminum plates using pitch-catch and cross-time frequency features [31]. For geometries relevant to fastener regions, Lamb-wave imaging has been demonstrated for corrosion around aluminum alloy hole edges, representative of rivet-hole corrosion [32]. FBG sensors have also proven to detect early corrosion-induced strain, monitor corrosion-related response in metallic structures, localize pitted

corrosion in coated or thermally sprayed metallic systems, and support corrosion detection using strain response through a two-level strategy [33–38]. Together, these studies support the technical feasibility of **Air SHIELD**'s sensing approach for capturing localized pitting corrosion and distributed corrosion thinning.

2.2.3 Air SHIELD for delamination in Composite Materials

Composite materials offer a high strength-to-weight ratio and significant structural efficiency benefits compared with metals. However, widespread adoption remains constrained by uncertainty in damage detection and lifecycle maintenance. Metals are ductile and often exhibit visible deformation or surface damage after loading events. In contrast, composites are susceptible to hidden damage mechanisms such as BVID, delamination, and matrix cracking, which increase inspection complexity and maintenance burden. Any out-of-plane stresses introduced to the composite panel will engage the weak axis of the laminate due to inherently poor through-thickness strength. Under these conditions, load transfer depends more heavily on the resin and fiber-matrix interface rather than the fibers themselves. Engineering design practices that minimize local out-of-plane stress concentrations help reduce the likelihood of delamination. However, these measures do not fully eliminate risk, particularly when damage originates from manufacturing defects or low-velocity impact events.

Studies have identified a dent decay phenomenon in which the visible indication of BVID gradually fades due to combined fatigue and aging effects, leaving the outer surface apparently pristine while internal damage remains present [39, 40]. **Air SHIELD** reduces this uncertainty through continuous strain-field measurements that do not depend on surface artifacts that may disappear over time. Unlike metals, where crack growth often follows established analytical relationships, composite damage progression is more complex because environmental exposure and operational variability alter intrinsic material properties, leading to less predictable behavior [40]. As a result, improved models for laminate stress prediction, delamination onset, and residual strength assessment remain an active research need. Although recent studies have advanced these predictive tools, key uncertainties persist, particularly regarding material variability and environmental effects [41–45]. **Air SHIELD** can address these gaps by providing high-resolution strain-field data for experimental validation and model calibration, enabling more reliable predictive and computational tools, reduces uncertainty, and improves confidence in composite structural performance throughout service life. Studies have examined the methods of measuring fatigue cracks using various sensing hardware, but these sensing system are strongly influenced by the placement and proximity to the crack [46–53]. Therefore, the proposed hybrid PZT-FBG Sensing Cluster enables global surface assessment rather than isolated strain measurement, which allows **Air SHIELD Detection** to evaluate the spatially distributed features to output accurate localization and early detection and classification of such subtle and inconspicuous damages.

2.2.4 Example Demonstration of Data Collection for Air SHIELD Optimizer using CRM Wingbox

A preliminary FEM study was conducted on the NASA Common Research Model (CRM) wingbox to generate representative strain-field data for **Air SHIELD** Optimizer. The CRM is a transonic transport vehicle benchmark provided by NASA for research use [54, 55]. The V15 wingbox model was analyzed in Femap using a static aeroelastic trim simulation to evaluate the strain distribution under cruise condition.

Damage scenarios were generated by defining an ellipsoidal region in the wingbox mesh and modifying the material properties of the elements inside that region. This provides a controlled numerical surrogate for localized material deterioration while allowing the damage location, size, and severity to be varied across simulations. Figure A.1 shows one example comparing the undamaged and damaged mid-plate strain fields. The solid line marks the deteriorated material region, while the dashed line marks a reference region away from the defect. Although the material change is applied locally, an obvious strain variation appears in the non-local reference region. This indicates that strain perturbations propagate through the coupled wingbox structure rather than remaining confined to the defect location.

The strain map of the damaged and undamaged wingbox are then used to synthesize readings at various

sensor sites in the network. The sensor features, containing the coordinates and orientation, are generated randomly for evaluation. A DeepSets encoder applies a multi-layer perceptron to each sensor vector and maps it into a single design vector that is permutation invariant [56]. That context conditions a normalizing flow, which applies a sequence of invertible deformations so a simple reference density becomes a flexible approximate posterior with a Gaussian distribution. BOED trains this model by minimizing the average probability density function for simulated true latent parameters, which is damage state or severity, from the generative model for many random designs and scenarios [25]. The objective of the BOED model is to minimize the posterior loss while maximizing EIG about the latent parameter. After training, sensor layouts are ranked by estimated EIG, with larger scores indicating more informative and optimal sensor placements.

2.3 Air SHIELD Detection: Machine Learning Architecture for Damage Classification

For damage classification, **Air SHIELD Detection** uses **Graph Neural Networks (GNNs)** as the primary machine learning architecture. Convolutional neural networks are widely used for damage detection [57, 58], but their reliance on regular Euclidean grids limits generalization to realistic structural geometries. GNNs address this limitation by operating directly on non-Euclidean domains, representing sensors as nodes and their physical or spatial relationships as edges. Through message passing, GNNs aggregate information in a geometry-consistent way, making them consistent with realistic damage propagation pattern [59–61]. Recent studies demonstrate strong SHM performance using GNNs, including high detection and localization accuracy on realistic aircraft structures [62–64].

To construct inputs for the GNN, sensor locations and recorded data for each node are mapped into a graph representation by a Graph Mapping Function. Sensor coordinates are projected onto the nearest points on the mesh. The node feature of each sensor reading is obtained by weighted interpolation of the associated surface mesh vertex data. Adjacency weights between sensors are computed based on the pseudo-geodesic distance between their projected points along the surface mesh, with weights decaying with distance.

The proposed framework has two GNN architectures, as illustrated in Fig. A.3. The first GNN performs global damage detection at the graph level. If damage is detected, the second GNN is used to perform damage localization and damage type classification. The damage detection network uses three stacked Graph Convolutional Network (GCN) layers with ReLU activation and Dropout regularization [59, 65, 66]. Global max pooling is applied to capture salient node responses, enabling rapid global damage detection. The pooled representation is mapped to a scalar through a fully connected layer, and sigmoid activation function maps it to the damage probability. As a binary classification task, the network is trained using Binary Cross-Entropy loss [67]. The second GNN performs point-wise damage type and localization classification. Since the updated node embeddings are defined on sensor nodes and their dimensionality does not match the point-cloud's, the embeddings are interpolated onto the surface point cloud. Specifically, for each point, features are obtained by geodesic-distance–weighted interpolation of the neighboring sensor embeddings, yielding a point-wise embedding consistent with the point-cloud size. Additional GCN layers are then applied.

A Multi-Layer Perceptron maps the embeddings to two outputs: overall damage probability (or severity) and probability of each damage type [68]. The network is trained using a two-part loss function. Damage localization is supervised by aligning the predicted damage distribution with a target distribution constructed from simulated damage locations, using Jensen–Shannon divergence [69, 70]. Damage type classification is supervised using a masked cross-entropy loss, applied only at points where the predicted damage probability exceeds a predefined threshold. The total loss is the weighted sum of these two terms.

3 Concept of Operations

To support smooth transition across departments without prior experience in sensor data analysis, this ecosystem builds on established digital platforms used by Airbus and Boeing. Strain data are interrogated from the **Air SHIELD Sensing Cluster** and processed using **Air SHIELD Detection**. Results are transferred to a centralized data repository and integrated into the shared platform. This workflow enables coor-

dinated decision-making and supports timely maintenance planning and inspection actions when required.

3.1 Data Pipeline and Connections

Onboard data transfer is organized into four hierarchical tiers. **Tier 1** focuses on hardware integration and data collection, including the **Air SHIELD Sensing Clusters**, interrogator, and micro-controller unit (MCU). Based on a scheduled or event based trigger, the MCU initiates PZT excitation and interrogator acquisition. The interrogator and MCU function as the cluster head and convert raw sensor signals into processed strain data. **Tier 2**, a communication point, connects each cluster head to the data processing module. Data are forwarded to **Tier 3**, which performs damage evaluation and system level decision making. When outputs exceed predefined thresholds, the system logs the data, issues a cockpit alert, and transmits the event to the airline maintenance server. During inspection, maintenance personnel verify the alert and schedule repair if Structural Repair Manual limits are exceeded. Following repair, a calibration burst establishes a new baseline for continued model operation. Processed results are stored in **Tier 4**, the central data repository, which archives sensor data, damage assessments, and structural response histories. These records support maintenance planning, parts availability, and long term use for structural analysis and aircraft design.

3.2 Overall Internal Software Integration

The **Air SHIELD** development for the sensor network requires minor changes to the overall Aircraft internal software onto the shared platform with other sensor networks. **Air SHIELD**'s in-flight systems use current onboard noncritical Ethernet systems to integrate data from the sensing clusters and transport it to the dashboard alert system and the flight data recorder. Data is then streamed over OEM health monitoring systems, for example Boeing's Aircraft Health Management [10] or Airbus' Skywise Health Monitoring [71]. Data is transported over the Aircraft Communications Addressing and Reporting System satellite [72].

Post-flight sensor data is automatically and wirelessly transmitted via the Quick Access Recorder to the airline data processing centers [72]. Pre-established predictive maintenance software, such as Aircraft Condition Monitoring System [73], is already a key predictive maintenance tool that **Air SHIELD** would onboard for analysis for individual system degradation. Boeing's Condition-Based Scheduled Maintenance or Airbus' Skywise Predictive Maintenance is the OEM's system for scheduling and cycling maintenance actions using data, leveraging AI and machine learning [74, 75]. This system sets the optimal maintenance and intervention recommendations based on predictive analysis and adjacent maintenance processes. Data provides airlines with actionable insights to maintain the airworthiness of their fleets.

3.3 Interoperability and Training

Deployment of **Air SHIELD** requires additions to Pilot Operating Handbook to integrate the **Air SHIELD** dashboard system alerts into standard procedures [76]. The airlines train pilots to handle the event of a detection by limiting flight maneuvers or declaring an emergency landing, thereby leading to safer flights.

Additions are required to both Boeing and Airbus' Aircraft Maintenance Manuals to integrate sensor maintenance, condition-based maintenance, procedures for detection events [77]. The Airliners and Maintenance Repair Training program trains maintenance crews for both the A and C checks for sensor repair. Data-driven by condition-based maintenance changes overall maintenance scheduling and location inspections. In the event of a detection, the airlines move the aircraft to unscheduled maintenance and then directly to heavy maintenance, where technicians locate the issue and begin repairs in accordance with sensor location detection. This workflow, shown in Fig.3.1, will be executed by expanding the existing health-monitoring platforms used by Airbus and Boeing.

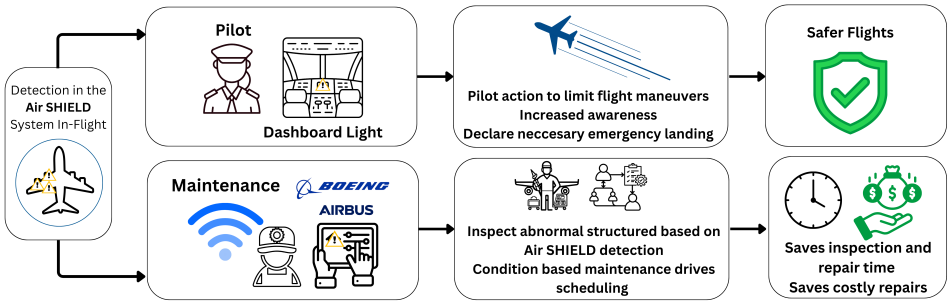

Figure 3.1: Operational workflow from in-flight anomaly detection to post-flight inspection and coordination

4 Path to deployment by 2035

Successful deployment in commercial aviation by 2035 requires a structured transition plan. Key elements include evaluation of the compliance with federal certification requirements, technology readiness level (TRL) of each subsystem, training for pilots and maintenance personnel, timeline with actionable plans, assessment of return on investment, and identification of technical and operational risks.

4.1 FAA Regulation and Training Requirements

For integration into commercial aviation structures, compliance to standards and regulations is required for approval and implementation into the industry as displayed in Fig. 4.1, which include specific standards and timeline based on the guidelines from official documents listed in [1, 78–89]

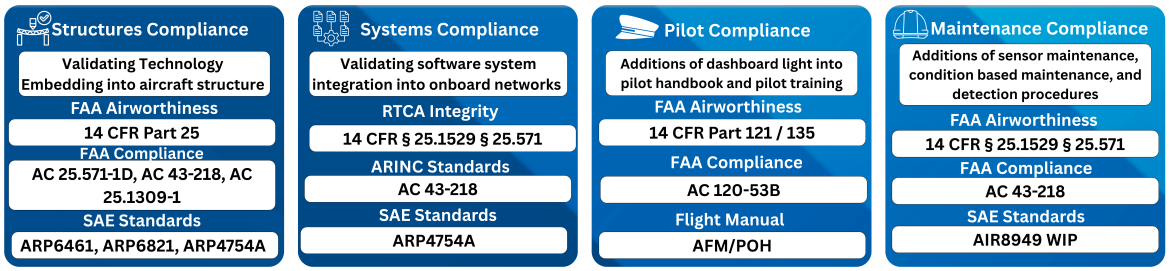

Figure 4.1: Standards and rules for approval

4.2 Technology Readiness Level

Table 4.1 summarizes the current TRL of each subsystem using the criteria defined in [90]. The primary development is **Air SHIELD Detection** model based on in-flight strain measurements. It must accurately detect damage initiation, track damage progression, and estimate structural life under operational loading conditions. In parallel, **Air SHIELD Sensing Cluster** requires validation through testing in a relevant flight environment. Completion of these items supports advancement of the full system to TRL 9 by 2035.

Subsystem	TRL	Current Status and Development Gaps
Air SHIELD Detection	3	Widely deployed across various applications. Development, training, and validating model for damage detection and localization using structural data is required to maintain detection accuracy.
PZT strips (**Sensing Cluster**)	4	PZT strips have been evaluated in controlled laboratory environments alongside FBG sensors. Further work requires refining sensor layout to ensure full surface coverage within effective sensing range.
Interrogation System	4	Waveform generation and signal interrogation hardware have been validated in laboratory settings. Integration and installation on aircraft platform are required to demonstrate operational readiness.

Subsystem	TRL	Current Status and Development Gaps
Air SHIELD Optimizer	4	Multiple methods have been reported in literature. Development and validation of our optimization framework is required to maximize probability of detection while ensuring complete structural coverage.
FBG sensor (**Sensing Cluster**)	6	FBG sensors have been demonstrated on existing aircraft structures and ground infrastructure. Additional validation through extended flight testing on commercial aircraft is required to advance to TRL 9.
User Interface	9	Established maintenance and monitoring platforms exist within Airbus and Boeing ecosystems. Additional development is required to integrate SHM outputs into these platforms for operational use.

Table 4.1: Current key technology subsystem capabilities and path to TRL advancement

4.3 Associated Risks and Mitigation

To ensure safety and reliability, risks associated with implementing **Air SHIELD** must be minimized. Risk and corresponding mitigation are detailed in Table 4.2 and evaluated based on likeliness (1-5) and severity (1-5).

Risk	Risk Level (Likelihood, Severity)	Mitigation
Sensor Failure	(4,5)	• Sensor Redundancy • Sensor Spacing FOS 2 • Rigorous Testing • Sensor Retrofit at D Check If Needed
Damage Positioned Where Lamb Waves Cannot Detect	(2,5)	• Sensor Redundancy • ML Model ensures detectability in all of structure • Sensor Placement Validated Computationally
ML Damage Detection Incorrectly Determines No Damage	(2,5)	• Periodic Sensor Structure Checks Between C checks • Rigorous Testing of ML Model
Damage In Irregular Location Not Expected By Model	(2,1)	• Sensor Redundancy • Sensor Spacing FOS 2 • Rigorously Tested ML Model
Software Failure When Detecting Damage	(2,3)	• Indicates Successful/Unsuccessful Scans To Operator

Low Risk
Med. Risk
High Risk

Table 4.2: Risk Table and Mitigation

4.4 Timeline

The timeline for implementing **Air SHIELD** spans from the present to 2035 detailing initial research to full industry implementation. In Fig. 4.2, the timeline is categorized into four primary development stages.

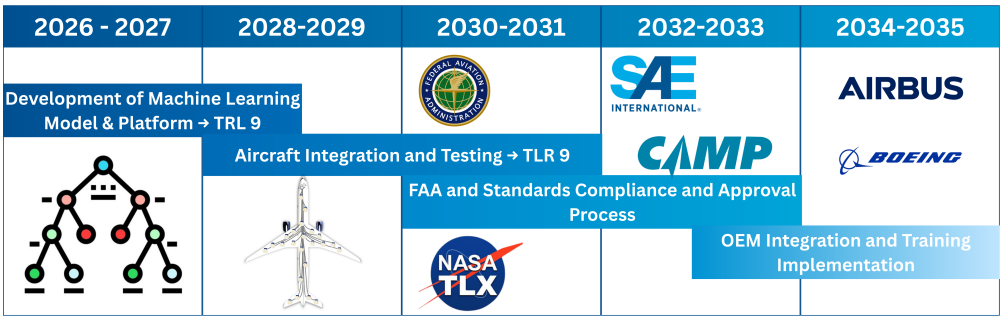

Figure 4.2: Estimated timeline with key action plans

4.5 Return on Investment

Success after deploying **Air SHIELD** is measured by cost savings. Cost serves as the primary metric as it reflects the long term viability of the technology. Lower maintenance cost supports sustained adoption across fleets. Reduced inspection time and improved operational efficiency also lower energy use during maintenance activities. Increased aircraft availability reduces fuel burn per revenue seat mile and lowers emissions, aligning with the objective of sustainable aviation. Implementing **Air SHIELD** on commercial aircraft improves efficiency of scheduled maintenance, specifically C check. During a C check, the interior aircraft seats and panels are removed, enabling maintenance crews to inspect the aircraft structure for cracks [91, 92]. The inspection process requires about 5 days for removing and reinstalling the aircraft interior. **Air SHIELD** replaces the need for visual inspection during C check, which greatly reduces labor cost by eliminating the man hours required for visual inspection [92]. The financial benefit gained from SHM's reduction in C check labor B_{Lbr} is a function of the man hours required for visual inspection and the hourly wage of aircraft maintenance technicians. Additionally, the C check duration is greatly decreased, allowing the aircraft to return to operation and earn revenue for the operator. The benefit of increased operation B_{Op} is a function of the operators profit per flight hour. The aircraft operator incurs a cost from implementing SHM systems on an aircraft. Cost can be broken down into sensor integration cost C_{int} and aircraft operation cost C_{Op} [91]. Both C_{int} and C_{Op} are functions of the sensors required, determined by the aircraft size. This is estimated from the total length of frames and stringers across the aircraft and detection range of the **Air SHIELD Sensing Cluster** [91].

When applied to a Boeing 737 NG, it is clear that the benefits of **Air SHIELD** far outweigh the incurred cost. Based on the fuselage parameters listed in Table A.2 in the Appendix, it is found that about 5000 sensors are required to detect the entire fuselage structure [93]. This includes FBG sensors and PZT placed using the SPO algorithm. This conservative estimate spaces sensors 20in apart, resulting in 100 % overlap between sensors. Assuming a cost of $24 per sensor, and an installation cost of $120,000, C_{int} is calculated. The benefit of labor is found by estimating the man hours required for visual fuselage structure inspection during the C check. The operational Benefit, B_{Op}, is the time saved during C check. The dollar amount of benefit gained from reduced time is dependent on the operator, and noted as + in the total benefit. Sample calculations for B777-200 and B737NG using FBG only in shown are Table A.3 and A.4 in the Appendix.

Cost		Benefit	
C_{SHM}	\$119,860	B_{Lbr}	\$856,800
C_{int}	\$120,000	B_{Op}	570 hr
C_{Op}	\$172,008		
C_{Total}	\$411,868	B_{Total}	\$856,800+

Table 4.3: Cost and Benefit of SHM System on 737 NG Using Hybrid FBG sensors and PZT

The increase in cost of operation is a function of the increase in mass from adding **Air SHIELD** based on a typical 737 NG flight of 900 nmi range. To estimate the additional mass of **Air SHIELD**, the selected hardware includes FBG sensors, PZT, an optical fiber switch, a PZT controller, a tunable laser, an optical circulator, a photodetector, and a digitizer and oscilloscope [94–101]. High frequency strain sampling with combined PZT actuation and FBG sensing requires more supporting hardware than an FBG only configuration. To limit system mass while preserving measurement fidelity, the proposed architecture adopts a zonal interrogation strategy. Rather than interrogating the full sensor network simultaneously with a dedicated hardware channel for each fiber, the architecture partitions the network into three interrogation zones. The multiplexing capability of FBG sensors supports allocation of 30 sensors per fiber. An optical switch and splitter sequentially route the optical source to zone 1, 2, and 3. This zonal interrogation approach reduces total interrogation hardware mass by a factor of 5.5. For the 737NG, the **Air SHIELD Sensing Clusters** result in a small weight addition of 183 lbs, or 0.2% increase in operating empty weight [93].

5 Demonstration of Air SHIELD using FBG Sensors

One critical capability of **Air SHIELD** is the ability to detect BVID on composite structures. As discussed in Section 2.2.3 and summarized in Table 2.1, BVID is among the most concerning composite damage modes as internal delamination and matrix cracking can significantly reduce residual strength while remaining visually inconspicuous. FBG provides the capability to detect BVID, which is typically impossible to locate via visual inspection [39, 40]. Difficulty detecting BVID has been a deterrent to the implementation of composite structures in commercial aviation, as operators and OEMs must account for inspection complexity, maintenance burden, and structural risk. By enabling continuous in-situ damage detection, **Air SHIELD** helps close this gap and supports confident use of composite aircraft structures [46–50].

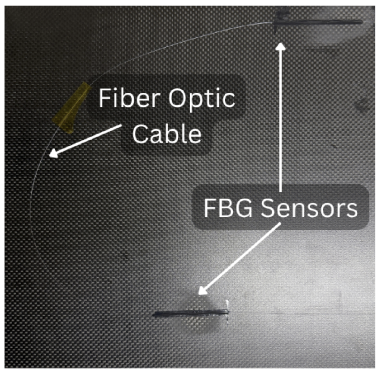

Figure 5.1: FBG installation on composite panel

To demonstrate the ability of FBG to detect and locate BVID, an experimental panel was constructed. A 3 mm x 12 in x 12 in isotropic quasi solid carbon fiber sheet, with 90 and 45 degree fabric schedules, was chosen to be representative of a composite aircraft structure. Two HBK FS70FBG were installed on the panel, in accordance with the manufacturer specification [102]. The installation locations of each sensor were recorded and are used for data analysis. Figure 5.1 demonstrates the FBG on the composite panel.

To impart BVID to the composite panel, a 500 g weight is dropped onto the center of the panel from increasing heights [103]. A steel rule was used to measure the height which the weight was dropped from. The impact energy is measured in ft-lb and is the product of the weight and height from which the weight is dropped from. The impact energies tested are presented in A.5. In between each impact, data is collected from both FBG sensors. The wavelengths measured by the sensors is later analyzed to determine is BVID has occurred.

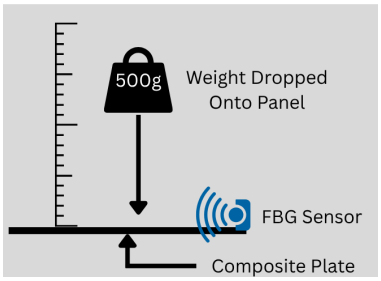

Figure 5.2: BVID Experimental Setup

To analyze the sensor readings and detect BVID, a baseline reading was taken first. The baseline showed that wavelengths between 1520.26 nm and 1530.26 nm indicated that BVID had not occurred. Next, wavelengths are recorded after each impact test. A wavelength outside of the baseline reading band indicates that BVID has occurred. This was repeated for all data sets. In Figure A.4, it is clear that wavelength readings increased following more energetic impacts, signifying that BVID has occurred. Ultimately, this experiment successfully demonstrates **Air SHIELD**'s ability to detect BVID on composite materials.

6 Conclusion

Air SHIELD, a revolutionary and autonomous SHM technology, is designed to improve aircraft safety and reduce operating costs while supporting continuous structural state awareness. The system integrates advanced sensing, physics-based simulation, and learning-based inference to enable early damage detection, localization, and classification. It improves decision making efficiency and supports condition-based inspection strategies across the aircraft life cycle. Case studies illustrate that the addition of **Air SHIELD** saves $9.13 per flight hour by reducing maintenance costs. Across the aircraft's operational lifetime, the system saves the operator $444,932 while also increasing the aircraft's utilization by 570 hours. BVID was also sucessfully detected on a composite plate using FBG sensors. A systematic development and validation timeline supports progressive risk reduction and system maturation. Based on the defined architecture, modeling fidelity, and deployment strategy, the technology aligns with certification and operational constraints and supports transition to real-world aircraft applications by 2035.

A Appendix

***** Expanded Analyses**
Additional research, modeling, and experiments have been incorporated throughout the technical report to address the judges' comments and present the topic in a more detailed, rigorous, and cohesive manner. Below is a summary of the major updates made since the proposal submission.

- The team conducted a preliminary case study using the NASA CRM wingbox for the **Air SHIELD Optimizer**. The wingbox was used as the benchmark mesh for generating undamaged and damaged cases. Undamaged scenarios were simulated by applying load conditions based on FAA Part 25 load requirements. Damaged scenarios were simulated by locally reducing the Young's modulus of selected elements within the defined damage region. The BOED model used these results as ground truth data and produced a list of optimal sensor layouts after running a series of amortized machine learning models.
- Extensive research was completed to evaluate and highlight the benefits of utilizing **Air SHIELD Sensing Clusters** for detecting corrosion and delamination in composite materials.
- The team conducted an initial experiment to detect BVID through a series of drop tests that introduced damage at different energy levels on a composite panel instrumented with FBG sensors. Measurements from the FBG sensors successfully demonstrated the ability to detect damage in composite panels.

Damage Type	Description
Accidental Damage	Results from unplanned external events such as barely visible impact damage and bird strikes. These events introduce localized deformation or internal damage that degrades structural integrity and threatens airworthiness if undetected.
Environmental Deterioration	Includes corrosion, erosion, oxidation, and moisture absorption driven by atmospheric exposure and material composition. The presence of dissimilar materials, such as metals and carbon fiber composites, increases susceptibility to galvanic corrosion.
Fatigue Damage	Develops under cyclic loading, vibration, and fluctuating stress during flight operations. Progressive crack initiation and growth weaken structural components and raise the risk of catastrophic structural failure.

Table A.1: Representative Aircraft Damage Type and Descriptions

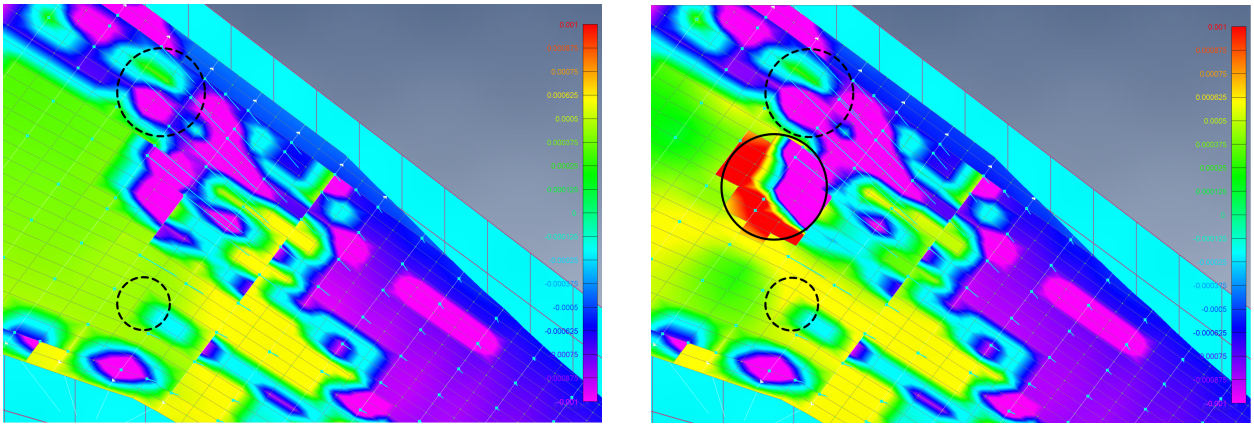

(a) Undamaged case (b) Damaged case, $r_E = 0.7$

Figure A.1: Mid-plate strain comparison. The damaged case has decay factor of $r_E = 0.7$. The solid line marks the local deteriorated material region, while the dashed lines mark some non-local reference regions where strain variation is observed.

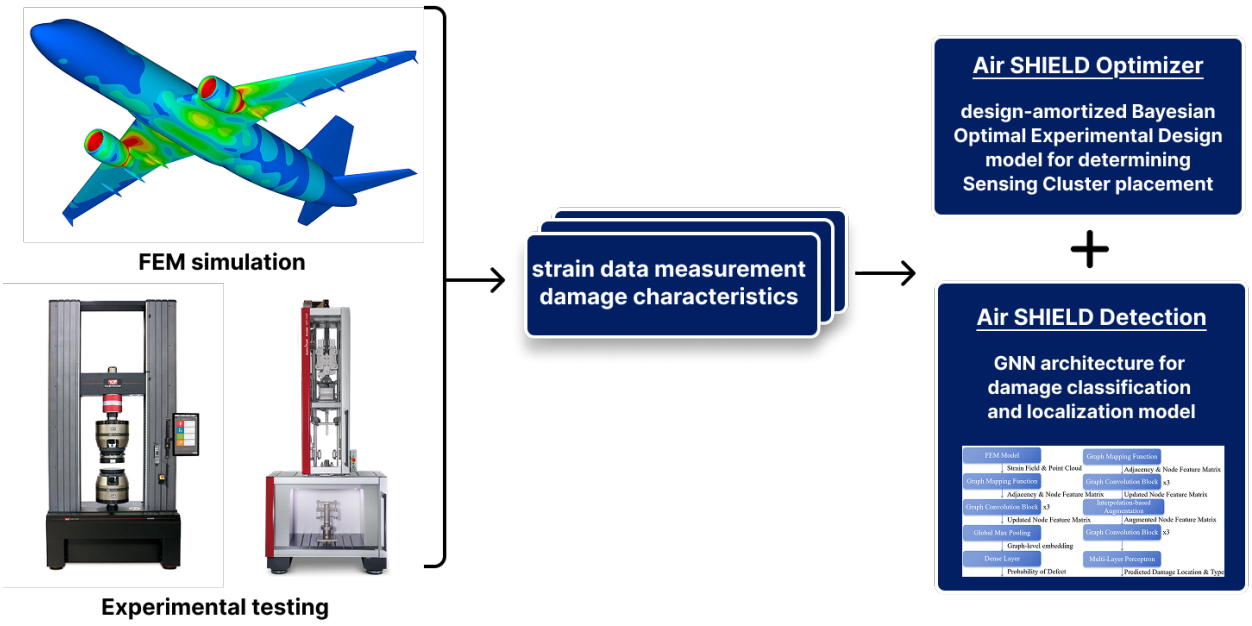

Figure A.2: Visual representation of inputs and outputs for **Air SHIELD** Detection model

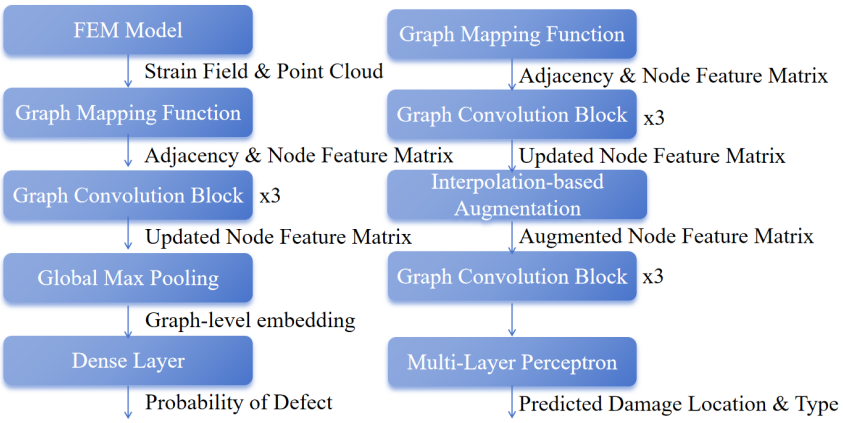

Figure A.3: Architecture of the proposed GNN framework: global damage detection (left) and damage localization and classification (right).

To calculate the required amount of **Air SHIELD Sensing Clusters**, the following assumptions and calculations were performed, based on a 737NG aircraft, with relationships highlighted in Eq. 1, 2, and 3.

Parameter	**Value**
Number of Frames (n_{frames})	60
Number of Stringers ($n_{\text{stringers}}$)	60
Fuselage Diameter (D_{frames})	148 in
Fuselage Length ($L_{\text{stringers}}$)	1200 in
Sensor Spacing (S_{cluster})	20 in

Table A.2: Fuselage Design and Sensor Spacing Parameters

$$L_{\text{total}} = n_{\text{frames}} \times D_{\text{frames}} \times \pi + n_{\text{stringers}} \times L_{\text{stringers}} \tag{1}$$

$$L_{\text{total}} = 60 \times 148 \times \pi + 60 \times 1200 \approx 99{,}897 \text{ in} \tag{2}$$

$$n_{\text{clusters}} = \frac{L_{\text{total}}}{S_{\text{cluster}}} = \frac{99{,}897}{20} \approx 4{,}995 \tag{3}$$

	Cost		**Benefit**
C_{SHM}	\$332,040	B_{Lbr}	\$906,667
C_{int}	\$120,000	B_{Op}	278 hr
C_{Op}	\$454,158		
C_{Total}	\$906,198	B_{Total}	\$906,667+

Table A.3: Cost and Benefit of SHM System on B777-200

The combination of FBG and PZT sensors is critical to the positive return on investment of **Air SHIELD**. In a case where a SHM system is made with only FBG sensors, the cost of acquisition and operation greatly increase, resulting in a cost of $8,000,000 across the aircraft's lifetime, while only yielding a benefit of $856,000.

	Cost		**Benefit**
C_{SHM}	$6,147,528	B_{Lbr}	$856,800
C_{int}	$120,000	B_{Op}	570 hr
C_{Op}	$1,879,872		
C_{Total}	$8,147,400	B_{Total}	$856,800+

Table A.4: Cost and Benefit of SHM System on 737 NG Using Only FBG

Weight (lb)	Height (ft)	Impact Energy (ft-lb)
1.1	0	0
1.1	0.0417	0.046
1.1	0.25	0.275
1.1	0.5	0.55
1.1	0.75	0.825
1.1	1.0	1.1

Table A.5: BVID Impact Energy

Figure A.4: BVID Wavelengths vs Baseline

References

[1] *Part 25 Airworthiness Standards: Transport Category Airplanes*. Tech. rep. Federal Aviation Administration.

[2] Airlines for America. *Operator/Manufacturer Scheduled Maintenance Volume 1 - Fixed Wing Aircraft (MSG-3), Revision 2022.1*. Tech. rep. Washington, DC: Airlines for America, 2023.

[3] Elena Jasiūnienė Markus G. R. Sause. *Structural Health Monitoring Damage Detection Systems for Aerospace*. Springer Cham, 2021. DOI: https://doi.org/10.1007/978-3-030-72192-3.

[4] Bruno Brandoli et al. "Aircraft Fuselage Corrosion Detection Using Artificial Intelligence". In: *Sensors* 21.12 (2021). ISSN: 1424-8220. DOI: 10.3390/s21124026. URL: https://www.mdpi.com/1424-8220/21/12/4026.

[5] Cecilia Perez Gago et al. "A Study of Pilot Response to System Failure in Transport Category Aircraft from 2000 to 2024". In: *2025 AIAA DATC/IEEE 44th Digital Avionics Systems Conference (DASC)*. 2025, pp. 1–8. DOI: 10.1109/DASC66011.2025.11257195.

[6] Airbus. *A Statistical Analysis of Commercial Aviation Accidents 1958-2020*. Tech. rep. 2021.

[7] Federal Aviation Administration. *Boeing 737-200: Aloha Airlines Flight 243, N73711*. 2022. URL: https://www.faa.gov/lessons_learned/transport_airplane/accidents/N73711.

[8] Iain G Hebden, Anthony M Crowley, and Wayne Black. "Overview of the F-35 Structural Prognostics and Health Management System". In: *e-Journal of Nondestructive Testing* 23.11 (2018). URL: https://www.ndt.net/?id=23392.

[9] William Bernard and Anthony Hoffmann. "SKYWISE - Big data platform as a foundation of airlines predictive andhealth monitoring". In: *4th Asia Pacific Conference of the Prognostics and Health Management*. 2023.

[10] Alex Leung and Stephen P. Miller. *Digital Aviation Solutions – Predictive Maintenance Ecosystem Overview*. https://services.boeing.com/bgsmedias/sys_master/root/hc6/h1b/8897529937950/C129-Predictive-Maintenance-Ecosystem-Overview-Stephen-Miller-and-Alex-Leung.pdf. Accessed: 2026–01-05. 2023.

[11] Justin Sindewald, Darren Macer, and Rhonda Walthall. *Predictive Maintenance in Aviation Panel*. https://phm2023.phmsociety.org/wp-content/uploads/sites/13/2023/11/Panel02-202311-PdM-PHM-Panel-Teubert.pdf. Accessed: 2026–01-05. 2023.

[12] Toshimichi Ogisu et al. "Damage growth detection of composite laminate using embedded FBG sensor/PZT actuator hybrid system". In: *Smart Sensor Technology and Measurement Systems*. Vol. 5758. Smart Structures and Materials. 2005. DOI: 10.1117/12.598085.

[13] Tomasz Wandowski et al. "A hybrid PZT-FBG sensing-based damage detection". In: *Health Monitoring of Structural and Biological Systems XVIII*. Vol. 12951. International Society for Optics and Photonics. 2024. DOI: 10.1117/12.3011986. URL: https://doi.org/10.1117/12.3011986.

[14] Qi Wu, Yoji Okabe, and Fengming Yu. "Ultrasonic Structural Health Monitoring Using Fiber Bragg Grating". In: *Sensors* 18.10 (2018). ISSN: 1424-8220. DOI: 10.3390/s18103395. URL: https://www.mdpi.com/1424-8220/18/10/3395.

[15] K. Hiramoto, H. Doki, and G. Obinata. "Optimal Sensor/Actuator Placement for Active Vibration Control Using Explicity Solution of Algebraic Riccati Equation". In: *Journal of Sound and Vibration* 229.5 (2000). URL: doi:10.1006/jsvi.1999.2530.

[16] Robert Frank Guratzsch. "Sensor Placement Optimization Under Uncertainty For Structural Health Monitoring Systems of Hot Aerospace Structures". PhD thesis. Vanderbilt University, 2007.

[17] Sahar Hassani and Ulrike Dackermann. "A Systematic Review of Optimization Algorithms for Structural Health Monitoring and Optimal Sensor Placement". In: *Sensors* 23.6 (2023). ISSN: 1424-8220. DOI: 10.3390/s23063293. URL: https://www.mdpi.com/1424-8220/23/6/3293.

[18] H Y Guo et al. "Optimal placement of sensors for structural health monitoring using improved genetic algorithms". In: *Journal of Smart Materials and Structures* (2004).

[19] Eric B. Flynn and Michael D. Todd. "A Bayesian approach to optimal sensor placement for structural health monitoring with application to active sensing". In: *Mechanical Systems and Signal Processing* 24.4 (2010), pp. 891–903. ISSN: 0888-3270. DOI: https://doi.org/10.1016/j.ymssp.2009.09.003. URL: https://www.sciencedirect.com/science/article/pii/S0888327009002635.

[20] William A. Maul et al. "Sensor Selection and Optimization for Health Assessment of Aerospace Systems". In: *Journal of Aerospace Computing, Information, and Communication* 5 (2008). DOI: 10.2514/1.34677. URL: https://doi.org/10.2514/1.34677.

[21] Z.Y. Shi, S.S. Law, and L.M. Zhang. "Optimum Sensor Placement for Structural Damage Detection". In: *Journal of Engineering Mechanics* 126.11 (Nov. 2000). DOI: 10.1061/(ASCE)0733-9399(2000)126:11(1173).

[22] Richard G. Cobb and Brad S. Liebst. "Sensor Placement and Structural Damage Identification from Minimal Sensor Information". In: *AIAA Journal* 35.2 (Feb. 1997). URL: https://doi.org/10.2514/2.103.

[23] Daniel C. Kammer. "Sensor placement for on-orbit modal identification and correlation of large space structures". In: *Journal of Guidance, Control, and Dynamics* 14.2 (1991), pp. 251–259. DOI: 10.2514/3.20635.

[24] Yichao Yang et al. "An optimal sensor placement design framework for structural health monitoring using Bayes risk". In: *Mechanical Systems and Signal Processing* 168 (2022), p. 108618. ISSN: 0888-3270. DOI: https://doi.org/10.1016/j.ymssp.2021.108618. URL: https://www.sciencedirect.com/science/article/pii/S0888327021009481.

[25] Noble Kennamer, Steven Walton, and Alexander Ihler. "Design Amortization for Bayesian Optimal Experimental Design". In: *The Thirty-Seventh AAAI Conference on Artificial Intelligence (AAAI-23)*. 2023.

[26] Adam Foster et al. *Variational Bayesian Optimal Experimental Design*. 2020. arXiv: 1903.05480 [stat.ML]. URL: https://arxiv.org/abs/1903.05480.

[27] William P. Winfree, Noreen A. Cmar-Mascis, and F. Raymond Parker. *Enhanced Imaging of Corrosion in Aircraft Structures with Reverse Geometry X-ray*. Tech. rep. NASA Langley Research Center, 2000.

[28] K. Teramoto and M. S. Rabbi. "Image Reconstruction of Corrosion under Coating Film by Dynamic Shear Strain Analysis of Lamb Waves". In: *19th World Conference on Non-Destructive Testing*. 2016.

[29] W. Zhu et al. "Ultrasonic Guided Wave NDT for Hidden Corrosion Detection". In: *Research in Nondestructive Evaluation* 10 (1998), pp. 205–225. DOI: 10.1007/PL00003908.

[30] M. Z. Silva, R. Gouyon, and F. Lepoutre. "Hidden Corrosion Detection in Aircraft Aluminum Structures Using Laser Ultrasonics and Wavelet Transform Signal Analysis". In: *Ultrasonics* 41.4 (2003), pp. 301–305. DOI: 10.1016/S0041-624X(02)00455-9.

[31] Lingyu Yu et al. “Corrosion Detection with Piezoelectric Wafer Active Sensors Using Pitch-Catch Waves and Cross-Time-Frequency Analysis”. In: *Structural Health Monitoring* 11.1 (2012), pp. 83–93. DOI: 10.1177/1475921711406580.

[32] Wei Dai et al. “Corrosion Monitoring Method of Porous Aluminum Alloy Plate Hole Edges Based on Piezoelectric Sensors”. In: *Sensors* 19.5 (2019), p. 1106. DOI: 10.3390/s19051106.

[33] C. H. Tan et al. “Fiber Bragg Grating Based Sensing System: Early Corrosion Detection for Structural Health Monitoring”. In: *Sensors and Actuators A: Physical* 246 (2016), pp. 123–128. DOI: 10.1016/j.sna.2016.04.028.

[34] Isabela Sousa et al. “Sensing System Based on FBG for Corrosion Monitoring in Metallic Structures”. In: *Sensors* 22.16 (2022), p. 5947. DOI: 10.3390/s22165947.

[35] Ying Huang et al. “Two-Dimensional Pitted Corrosion Localization on Coated Steel Based on Fiber Bragg Grating Sensors”. In: *Journal of Civil Structural Health Monitoring* 10 (2020), pp. 927–945. DOI: 10.1007/s13349-020-00424-1.

[36] Fodan Deng et al. “Pitted Corrosion Detection of Thermal Sprayed Metallic Coatings Using Fiber Bragg Grating Sensors”. In: *Coatings* 7.3 (2017), p. 35. DOI: 10.3390/coatings7030035.

[37] Luyang Xu, Dawei Zhang, Ying Huang, et al. “Monitoring Epoxy Coated Steel under Combined Mechanical Loads and Corrosion Using Fiber Bragg Grating Sensors”. In: *Sensors* 22.20 (2022), p. 8034. DOI: 10.3390/s22208034.

[38] Yuyao Cheng et al. “Application of a Novel Long-Gauge Fiber Bragg Grating Sensor for Corrosion Detection via a Two-Level Strategy”. In: *Sensors* 19.4 (2019), p. 954. DOI: 10.3390/s19040954.

[39] Jerzy Komorowski, Ronald Gould, and David Simpson. “Synergy between Advanced Composites and New NDI Methods”. In: *Advanced Performance Materials* 5 (Jan. 1998), pp. 137–151. DOI: 10.1023/A:1008694223117.

[40] J. Rouchon. *Fatigue and Damage Tolerance Evaluation of Structures: The Composite Materials Response*. Tech. rep. NLR-TP-2009-221. National Lucht-en Ruimtevaartlaboratorium (NLR), 2009.

[41] Paul W. Harper and Stephen R. Hallett. “A fatigue degradation law for cohesive interface elements – Development and application to composite materials”. In: *International Journal of Fatigue* 32.11 (2010), pp. 1774–1787. ISSN: 0142-1123. DOI: https://doi.org/10.1016/j.ijfatigue.2010.04.006. URL: https://www.sciencedirect.com/science/article/pii/S0142112310000988.

[42] Luiz F. Kawashita and Stephen R. Hallett. “A crack tip tracking algorithm for cohesive interface element analysis of fatigue delamination propagation in composite materials”. In: *International Journal of Solids and Structures* 49.21 (2012), pp. 2898–2913. ISSN: 0020-7683. DOI: https://doi.org/10.1016/j.ijsolstr.2012.03.034. URL: https://www.sciencedirect.com/science/article/pii/S0020768312001369.

[43] “Numerical analysis of delamination buckling and growth in slender laminated composite using cohesive element method”. In: *Computational Materials Science* 50.1 (2010), pp. 20–31. ISSN: 0927-0256. DOI: https://doi.org/10.1016/j.commatsci.2010.07.003. URL: https://www.sciencedirect.com/science/article/pii/S0927025610004118.

[44] Andrea Sellitto et al. “Mixed-Mode Delamination Growth Prediction in Stiffened CFRP Panels by Means of a Novel Fast Procedure”. In: *Applied Sciences* 9.22 (2019). ISSN: 2076-3417. DOI: 10.3390/app9224761. URL: https://www.mdpi.com/2076-3417/9/22/4761.

[45] Alireza Taherzadeh-Fard et al. “Numerical Analysis of Damage in Composites: From Intra-Layer to Delamination and Data-Assisted Methods”. In: *Mathematics* 13.10 (2025). ISSN: 2227-7390. DOI: 10.3390/math13101578. URL: https://www.mdpi.com/2227-7390/13/10/1578.

[46] Victor Giurgiutiu, Andrei Zagrai, and Jing Jing Bao. “Piezoelectric Wafer Embedded Active Sensors for Aging Aircraft Structural Health Monitoring”. In: *Structural Health Monitoring* 1.1 (2002), pp. 41–61. DOI: 10.1177/147592170200100104.

[47] Victor Giurgiutiu, Andrei Zagrai, and Jingjing Bao. “Damage Identification in Aging Aircraft Structures with Piezoelectric Wafer Active Sensors”. In: *Journal of Intelligent Material Systems and Structures* 15.9–10 (2004), pp. 673–687. DOI: 10.1177/1045389X04038051.

[48] Jingjing He et al. “A Multi-Feature Integration Method for Fatigue Crack Detection and Crack Length Estimation in Riveted Lap Joints Using Lamb Waves”. In: *Smart Materials and Structures* 22.10 (2013), p. 105007. DOI: 10.1088/0964-1726/22/10/105007.

[49] Frank H. G. Stolze et al. “Fatigue-Crack Detection in a Multi-Riveted Strap-Joint Aluminium Aircraft Panel Using Amplitude Characteristics of Diffuse Lamb Wave Field”. In: *Materials* 16.4 (2023), p. 1619. DOI: 10.3390/ma16041619.

[50] Sean K. Chilelli, Joseph J. Schomer, and Marcelo J. Dapino. “Detection of Crack Initiation and Growth Using Fiber Bragg Grating Sensors Embedded into Metal Structures through Ultrasonic Additive Manufacturing”. In: *Sensors* 19.22 (2019), p. 4917. DOI: 10.3390/s19224917.

[51] Yan Zhao et al. “The Location Monitoring of Fatigue Crack Damage by Using the Spectral Area Extracted from FBG Spectra”. In: *Sensors* 20.8 (2020), p. 2375. DOI: 10.3390/s20082375.

[52] D. C. Betz et al. “Multi-Functional Fibre Bragg Grating Sensors for Fatigue Crack Detection in Metallic Structures”. In: *Proceedings of the Institution of Mechanical Engineers, Part G: Journal of Aerospace Engineering* 220.5 (2006), pp. 453–461. DOI: 10.1243/09544100JAERO34.

[53] Magdalena Mieloszyk. “Fatigue Crack Propagation Monitoring Using Fibre Bragg Grating Sensors”. In: *Vibration* 4.3 (2021), pp. 700–721. DOI: 10.3390/vibration4030039.

[54] NASA Langley Research Center. *Geometry — NASA Common Research Model*. https://commonresearchmodel.larc.nasa.gov/geometry/. Accessed: 2026-05-01.

[55] NASA Langley Research Center. *Common Research Model (CRM) Wingbox Finite Element Models: Wingbox Models Description*. https://commonresearchmodel.larc.nasa.gov/wp-content/uploads/sites/7/2014/02/CRM_wingboxFEM_description_1.pdf. Accessed: 2026-05-01.

[56] Manzil Zaheer et al. “Deep Sets”. In: *arXiv preprint arXiv:1703.06114* (2017). DOI: 10.48550/arXiv.1703.06114. URL: https://doi.org/10.48550/arXiv.1703.06114.

[57] Mahindra Rautela and S Gopalakrishnan. “Ultrasonic guided wave based structural damage detection and localization using model assisted convolutional and recurrent neural networks”. In: *Expert Systems with Applications* 167 (2021), p. 114189.

[58] Tianrui Huang et al. “A hybrid deep learning framework based on diffusion model and deep residual neural network for defect detection in composite plates”. In: *Applied Sciences* 13.10 (2023), p. 5843.

[59] TN Kipf. “Semi-supervised classification with graph convolutional networks”. In: *arXiv preprint arXiv:1609.02907* (2016).

[60] Michael M Bronstein et al. “Geometric deep learning: going beyond euclidean data”. In: *IEEE Signal Processing Magazine* 34.4 (2017), pp. 18–42.

[61] Zonghan Wu et al. “A comprehensive survey on graph neural networks”. In: *IEEE transactions on neural networks and learning systems* 32.1 (2020), pp. 4–24.

[62] Margaret Sullivan Pepe. “Receiver operating characteristic methodology”. In: *Journal of the American Statistical Association* 95.449 (2000), pp. 308–311.

[63] Emiliano Del Priore and Luca Lampani. “Real-time damage detection and localization on aerospace structures using graph neural networks”. In: *Journal of Sensor and Actuator Networks* 14.5 (2025), p. 89.

[64] Giannis Stamatelatos et al. “Graph neural networks for SHM: exploiting spatial interdependencies of strain data for diagnostics and prognostics”. In: *Structural Health Monitoring* (2025), p. 14759217251386802.

[65] Jie Zhou et al. “Graph neural networks: A review of methods and applications”. In: *AI open* 1 (2020), pp. 57–81.

[66] Nitish Srivastava et al. “Dropout: a simple way to prevent neural networks from overfitting”. In: *The journal of machine learning research* 15.1 (2014), pp. 1929–1958.

[67] Anqi Mao, Mehryar Mohri, and Yutao Zhong. “Cross-entropy loss functions: Theoretical analysis and applications”. In: *International conference on Machine learning*. pmlr. 2023, pp. 23803–23828.

[68] Fionn Murtagh. “Multilayer perceptrons for classification and regression”. In: *Neurocomputing* 2.5-6 (1991), pp. 183–197.

[69] Jianhua Lin. “Divergence measures based on the Shannon entropy”. In: *IEEE Transactions on Information theory* 37.1 (2002), pp. 145–151.

[70] Jonathon Shlens. “Notes on kullback-leibler divergence and likelihood”. In: *arXiv preprint arXiv:1404.2000* (2014).

[71] Airbus. “Airbus Inflight health monitoring: For on-time dispatch”. In: *FAST technical articles* (July 2022). Product Support Manager, Airbus. URL: https://www.aircraft.airbus.com/sites/g/files/jlcbta126/files/2022-07/FAST-Health-Monitoring-layout.pdf (visited on 05/22/2024).

[72] Angela Saffin. *Post-Flight Analysis for Actionable Insights*. Presentation, Boeing Connect. Portfolio Leader, Flight Data Analytics. Sept. 2023.

[73] SKYbrary. *Aircraft Condition Monitoring System (ACMS)*. Accessed: May 22, 2024. EUROCONTROL, ICAO and Flight Safety Foundation. 2021. URL: https://skybrary.aero/articles/aircraft-condition-monitoring-system-acms.

[74] Boeing. *Condition-Based Scheduled Maintenance*. Technical White Paper. Boeing Global Services. 2024. URL: https://services.boeing.com/bgsmedias/sys_master/noindex/hf9/h02/9063559921694/Condition-Based-Scheduled-Maintenance/Condition-Based-Scheduled-Maintenance.pdf (visited on 05/22/2024).

[75] Airbus. *Skywise: The Aviation Data Platform*. Product Brochure. Airbus Services. 2019. URL: https://www.aircraft.airbus.com/sites/g/files/jlcbta126/files/6baf9195385c253a1553f6e2a656f92b_Skywise-brochure-2019.pdf (visited on 05/22/2024).

[76] Federal Aviation Administration. *Advisory Circular AC 25.1581-1: Airplane Flight Manual*. Change 1. U.S. Department of Transportation. Oct. 2012. URL: https://www.faa.gov/documentLibrary/media/Advisory_Circular/AC%2025.1581-1.pdf (visited on 05/22/2024).

[77] Federal Aviation Administration. *Advisory Circular AC 43-218: Procedures for Gaining Maintenance or Inspection Credit from Use of Equipment and/or Health Monitoring Systems*. AFS-300. U.S. Department of Transportation. Jan. 19, 2023. URL: https://www.faa.gov/documentLibrary/media/Advisory_Circular/AC_43-218_FAA_Web.pdf (visited on 05/22/2024).

[78] Federal Aviation Administration. *Advisory Circular 25.571-1D: Damage Tolerance and Fatigue Evaluation of Structure*. Tech. rep. AC 25.571-1D. U.S. Department of Transportation, 2011. URL: https://www.faa.gov/regulations_policies/advisory_circulars/index.cfm/go/document.information/documentid/865446.

[79] Federal Aviation Administration. *Pilot's Handbook of Aeronautical Knowledge: Chapter 9, Flight Manuals and Other Documents*. FAA-H-8083-25C. Accessed February 2026. U.S. Department of Transportation. 2023. URL: https://www.faa.gov/sites/faa.gov/files/11_phak_ch9.pdf.

[80] SAE International. *ARP4754A: Guidelines For Development Of Civil Aircraft and Systems*. Aerospace Recommended Practice ARP4754A. SAE International, Dec. 2010. DOI: 10.4271/ARP4754A.

[81] Michelle Lange. *DO-254 Overview, Pros, Cons, and Discussion*. Presented at the Military and Aerospace Programmable Logic Devices (MAPLD) Conference. Mentor Graphics Corporation. Available at: https://nepp.nasa.gov/mapld_2009/talks/083109_Monday/01_Lange_Michelle_mapld09_pres_1.pdf. Greenbelt, MD: NASA Electronic Parts and Packaging (NEPP) Program, Aug. 2009.

[82] SAE International. *ARP6461A: Guidelines for Implementation of Structural Health Monitoring on Fixed Wing Aircraft*. Aerospace Recommended Practice ARP6461A. Warrendale, PA: SAE International, Aug. 2021. DOI: 10.4271/ARP6461A. URL: https://www.sae.org/standards/arp6461a-guidelines-implementation-structural-health-monitoring-fixed-wing-aircraft.

[83] SAE International. *ARP6821: Guidance for Assessing the Damage Detection Capability of Structural Health Monitoring Systems*. Aerospace Recommended Practice ARP6821. Warrendale, PA: SAE International, Feb. 2025. DOI: 10.4271/ARP6821. URL: https://www.sae.org/standards/arp6821-guidance-assessing-damage-detection-capability-structural-health-monitoring-systems.

[84] SAE International. *ARP4754A: Guidelines for Development of Civil Aircraft and Systems*. Aerospace Recommended Practice ARP4754A. Warrendale, PA: SAE International, Dec. 2010. DOI: 10.4271/ARP4754A. URL: https://www.sae.org/standards/arp4754a-guidelines-development-civil-aircraft-systems.

[85] Federal Aviation Administration. *Air Carrier Certification*. U.S. Department of Transportation. Accessed: 2024-05-22. 2024. URL: https://www.faa.gov/licenses_certificates/airline_certification/air_carrier.

[86] Federal Aviation Administration. *135 Certification: Air Carrier and Commercial Operator*. U.S. Department of Transportation. Accessed: 2024-05-22. 2024. URL: https://www.faa.gov/licenses_certificates/airline_certification/135_certification.

[87] Federal Aviation Administration. *Advisory Circular AC 120-53B: Guidance for Conducting and Use of Flight Standardization Board Evaluations*. Advisory Circular AC 120-53B. Includes Change 1. Note: Cancelled by AC 120-53C as of September 2025. Washington, DC: U.S. Department of Transportation, Nov. 2013. URL: https://www.faa.gov/regulations_policies/advisory_circulars/index.cfm/go/document.information/documentID/1022507.

[88] SAE International. *AIR8949: Guidance for Training Personnel Associated with the Installation and Usage of SHM Systems*. Aerospace Information Report AIR8949. Warrendale, PA: SAE International, Sept. 2024. URL: https://www.sae.org/standards/air8949-guidance-training-personnel-associated-installation-usage-shm-systems.

[89] Parasoft Corporation. *DO-178C Software Compliance for Aerospace & Defense*. Ebook. Accessed: 2024-05-22. Parasoft, 2023. URL: https://alm.parasoft.com/hubfs/ebook-DO-178C-Software-Compliance-Aerospace-Defense.pdf.

[90] National Aeronautics and Space Administration. *Technology Readiness Levels*. Accessed January 2026. 2023. URL: https://www.nasa.gov/directorates/somd/space-communications-navigation-program/technology-readiness-levels/.

[91] Ting Dong and Nam H. Kim. "Cost-Effectiveness of Structural Health Monitoring in Fuselage Maintenance of the Civil Aviation Industry †". In: *Aerospace* 5.3 (2018). DOI: 10.3390/aerospace5030087.

[92] Vincenzo et al. Cusati. "Impact of Structural Health Monitoring on Aircraft Operating Costs by Multidisciplinary Analysis". In: *Sensors* 21.20 (2021). DOI: 10.3390/s21206938.

[93] Boeing. *737 Next-Generation Passenger Characteristics*. Accessed: Jan. 16, 2026. Startup Boeing. URL: https://www.boeing.com/content/dam/boeing/boeingdotcom/company/about_bca/startup/pdf/historical/737NG_passenger.pdf.

[94] FBGS. *Draw Tower Gratings Fiber Optics Sensor*. Accessed January 2026. URL: https://fbgs.com/components/draw-tower-gratings-dtgs/.

[95] Acellent Technologies. *SMART Layer Sensor System*. Accessed January 2026. 2024. URL: https://www.acellent.com/products/smart-layer-sensors.

[96] Agiltron. *MEMS Matrix 64x64 Optical Switch Specifications*. Accessed January 2026. 2023. URL: https://agiltron.com/dlc/specs/MEMS%20Matrix%2064x64%20Optical%20Switch.pdf.

[97] Acellent Technologies. *Structural Health Monitoring Hardware Products*. Accessed January 2026. 2024. URL: https://www.acellent.com/products/hardware.

[98] APEX Technologies. *Tunable Laser Source*. Accessed January 2026. URL: https://apex-t.com/tunable-laser-source/.

[99] Thorlabs. *6015-3-APC Fiber Optic Circulator*. Accessed January 2026. URL: https://www.thorlabs.com/item/6015-3-APC.

[100] Thorlabs. *FPD610-FC-NIR Free-Space Photodetector*. Accessed January 2026. 2024. URL: https://www.thorlabs.com/item/FPD610-FC-NIR.

[101] National Instruments. *PXIe-5110 High-Speed Digitizer*. Accessed January 2026. 2024. URL: https://www.ni.com/en-us/shop/model/pxie-5110.html.

[102] Hottinger Brüel & Kjaer GmbH. *Mounting Instructions: FS70FBG Array of Bare FBG*. Mat. DVS: A05395 03 E00 00. HBK FiberSensing, S.A. Darmstadt, Germany, Nov. 2022. URL: www.hbkworld.com.

[103] Andrew E. Lovejoy and Adam Przekop. "Imparting Barely Visible Impact Damage to a Stitched Composite Large-Scale Pressure Box". In: *57th AIAA/ASCE/AHS/ASC Structures, Structural Dynamics, and Materials Conference*. NASA Technical Report 20160007726. American Institute of Aeronautics and Astronautics, 2016. DOI: 10.2514/6.2016-2178.